Chemosphere 166 (2017) 334–342

Contents lists available at ScienceDirect

Chemosphere

journal homepage: www.elsevier.com/locate/chemosphere

Characterization of pH-fractionated humic acids derived from Chinese weathered coal

Shuiqin Zhang [a, b, 1], Liang Yuan [a, 1], Wei Li [a], Zhian Lin [a], Yanting Li [a], Shuwen Hu [b], Bingqiang Zhao [a, *]

[a] Key Laboratory of Plant Nutrition and Fertilizer, Ministry of Agriculture/Institute of Agricultural Resources and Regional Planning, Chinese Academy of Agricultural Sciences, Beijing 100081, China

[b] College of Resources and Environmental Sciences, China Agricultural University, Beijing 100193, China

HIGHLIGHTS

- Humic acids from Chinese weathered coal were pH-fractionated successfully.
- The compositional and structural characteristics of HA fractions were investigated.
- The characteristics of HA fractions varied with the extraction solution pH.
- HA$_{6\sim7}$ had the highest aromaticity and the most abundant COO/N-C=O groups.
- The nonprotonated carbon in HA fractions increased with the extraction solution pH.

ARTICLE INFO

Article history:
Received 12 July 2016
Received in revised form
20 September 2016
Accepted 21 September 2016
Available online 1 October 2016

Handling Editor: Xiangru Zhang

Keywords:
Chinese weathered coal
Humic acids
pH fractionation
Characterization

ABSTRACT

To reduce the compositional and structural heterogeneity of humic acids (HAs) and achieve better use of HA resources, in this study, we report a new sequential dissolution method for HAs derived from Chinese weathered coal. This method was used to separate HAs into seven fractions by adjusting the pH (3-10) of the extraction solution. The results showed that the HA fractions derived from Chinese weathered coal were concentrated up to 90.31% in the lower pH solutions (3-7). The compositional and structural characteristics of the HA fractions were determined by elemental analysis; ultraviolet–visible (UV-Vis), Fourier transform infrared (FTIR), and solid-state ^{13}C-nuclear magnetic resonance (NMR) spectroscopies; and other techniques. The results showed significant differences among the HA fractions. The concentrations of the total acidic groups and the carboxyl groups decreased with the increasing pH of the extraction solution. However, the HA fractions derived from extraction solutions with pH 3-4 had relatively lower aromaticity but a higher protonated carbon content. The HA fractions derived from extraction solutions with pH 6-7 had the highest aromaticity and the greatest abundance of COO/N-C=O. This study demonstrated that adjusting the pH of the extraction solution is one way to fractionate HAs from Chinese weathered coal and to obtain HA fractions with compositions and structures that could serve as useful material for study and utilization.

1. Introduction

Humic acids (HAs) are amorphous, colloidal and polydispersed organic compounds with complex compositions and structures resulting from chemical and biological degradation and the transformation of plant and animal residues and microbial cells (Hayes and Wilson, 1997; Dong et al., 2008). They are widely distributed in nature, and their composition, structure and usefulness for soil fertilization have been extensively investigated (Zheng, 1991; Stevenson, 1994). However, the high degree of heterogeneity in their compositions and origins have made their structures difficult to ascertain. Fractionation, especially by preparative high-performance size-exclusion chromatography, ultrafiltration, and precipitation, has been commonly employed to overcome this problem by reducing the heterogeneity of HAs to gain a better understanding of their composition and structure as well as their

---

Abbreviations: HAs, humic acids; UV-Vis, ultraviolet and visible; FTIR, Fourier transform infrared; NMR, nuclear magnetic resonance; CP/TOSS, cross polarization/total sideband suppression; DD, dipolar dephasing; PCA, principal component analysis.

[*] Corresponding author.
E-mail address: zhaobingqiang@caas.cn (B. Zhao).

[1] Indicates the authors who contributed equally to this study.

http://dx.doi.org/10.1016/j.chemosphere.2016.09.095

value for soil fertilization (Stevenson, 1994; Nardi et al., 2002, 2007; Mao et al., 2007; Dong et al., 2008, 2009; Asakawa et al., 2008; Canellas et al., 2010; Klučáková and Kalina, 2015).

The dissociation of acid functional groups in extraction solutions with a set pH is a determining factor for HA isolation (Bakina and Orlova, 2012). When the pH of the extraction solution is very low, all of the acidic functional groups in the HAs are protonated, and the humic particles have no surplus charge, which makes them insoluble and allows for precipitation (Klučáková and Pekař, 2005). However, a stepwise increase of the extraction solution pH will introduce charges, and the HAs are dissolved out gradually, increasing their solubility and sequentially extracting different HA fractions (Kipton et al., 1992). The dissolution of HAs in solution at a lower pH takes more time to reach a steady state, and the dissolution rate of HAs at higher pH is considerably faster (Brigante et al., 2009). Therefore, precipitation by adjusting the pH of a pyrophosphate or NaOH-H_3PO_4-CH_3COOH-H_3BO_3 buffer solution is the accepted classical method and is well suited for a large-scale application (Stevenson, 1994; Fujitake et al., 1998; Klučáková and Kalina, 2015). A method first proposed by Stevenson (1994) verified that HAs are organic matter fractions soluble in solutions of neutral and alkaline pH but insoluble in acids. Based on this theory, Fujitake et al. (1998, 1999, 2003) fractionated HAs from different soil samples into six fractions by sequentially using HA-pyrophosphate solutions of increasing pH (3, 5, 7, 9, 11 and 13). Remarkable differences in the yields, spectral properties and particle sizes of the fractions were evident. They verified that the proportion of HA total yield extracted at acidic to neutral pH (3–7) was higher than the yield at alkaline pH (9–13) for most soil samples. They also showed that the particle size of HAs was positively correlated with pH. However, they showed that the shape of the UV–Vis and IR spectra was more dependent on the origin of the soil than the pH of the extraction solution and that the highest degree of humification was found in the neutral region. The HA extracted at a lower pH had more aromatic and carboxylic groups, whereas more aliphatic and/or peptide groups were present in the HA fractions extracted from higher pH solutions (Klučáková and Kalina, 2015). However, the high heterogeneity of the HAs and the complexity of the extracts complicated the fractionation process. Specifically, the heterogeneity of HAs impeded a thorough isolation, while the complexity of the extracts interfered with further studies on the HA fractions. Common extraction solutions, such as $NaNO_3$, $Na_4P_2O_7$ or NaOH-H_3PO_4-CH_3COOH-H_3BO_3, usually contain nitrogen (N), phosphorus (P), and other soil nutrients (Fujitake et al., 1998; You et al., 2006; Klučáková and Kalina, 2015). Thus, after pH-based fractionation, the HA fractions obtained are vulnerable to residual elements in the extraction solutions, leading to an incorrect assessment of their N and P contents that affects subsequent research. Therefore, the traditional extraction method must be improved to obtain fractions with greater gradation and to prevent extraneous elements from being introduced into the HA assay.

The structure and composition of HAs is highly dependent on their origin (Stevenson, 1994). The hydrothermal conditions under which HAs are produced, the formation period and many other external conditions affect their composition. Current research is concentrated on the characteristics of HAs derived from lignite, soil, and compost (Novák et al., 2015; Mao et al., 2007; Canellas et al., 2010), and significant information, including information about their diverse composition and conformation, has been collected for these source materials.

Weathered coal is the product of coal oxidized by air and water and usually exists at the surface of a coal seam or is buried under a thin layer of coal in a coal seam. Due to its high degree of oxidization, the HAs derived from weathered coal are expected to have quite different compositional, structural and physicochemical properties than HAs of other origins, especially in the content and structural features of the aromatic carbons (Zheng, 1991; Stevenson, 1994). In addition, the aromatic features of HAs can be probed using a long-range dipolar dephasing technique (Mao et al., 2010). The available data indicate that an abundant reserve of weathered coal exists (~100 billion tons in China alone). However, the high oxygen content and low calorific value of weathered coal make it unsuitable as a fuel for power generation or as a coking coal; however, the extraction rate of HAs from weathered coal is similar to that from lignite and peat (He et al., 2003). He et al. (2003) reported that the acidic functional group content of HAs from weathered coal, lignite and peat varies only slightly. Zheng (1991) also indicated that the HAs derived from weathered coal have a higher content of carboxyl groups and other acidic functional groups than lignite and peat. The high content of aromatic and acidic functional groups implies that weathered coal is potentially a good source of HAs for agriculture (Zheng, 1991; Li et al., 2012). However, to the best of our knowledge, the characteristics of HAs derived from weathered coal have not been investigated to the same extent as those derived from other sources.

In this paper, we report a new sequential dissolution and extraction process for HAs that use extraction solutions containing dilute NaOH and HCl in various proportions with pHs ranging from 3 to 10 and on the structural and compositional characteristics of the HA fractions obtained by an elemental composition determination, UV–Vis, FTIR, and solid-state ^{13}C-NMR analyses. The main objective of this research was the isolation and characterization of the various HA fractions from weathered coal, a comparison of their differences and an eventual analysis of their effective use for soil fertilization.

2. Materials and methods

2.1. Materials

The weathered coal was collected from Huolinhe (E 119°15′, N 45°23′; Tongliao, Inner Mongolia Autonomous Region, Northeast China), which has a temperate continental climate. Conifers and Ginkgoales from the Late Jurassic are the main coal-forming plants, and cycads and ferns have also been detected in coal samples (Mei and Cui, 1994). Gymnospermous fossils have been discovered in the coal stratum. The total HAs and ash contents of the weathered coal are 50.94% and 36.26%, respectively. The carbon (C), oxygen (O), hydrogen (H) and nitrogen (N) contents are 35.15%, 0.80%, 4.52%, and 23.27%, respectively.

2.2. Fractionation of HA from Chinese weathered coal

The HA extraction and fractionation procedure in this study is a modification of the traditional alkali extraction method (Stevenson, 1994; Yuan et al., 2015). This process is more conducive to industrial practice for a large volume extraction. The fractionation procedure was conducted via the sequential steps shown in Fig. 1. Weathered coal and 1 M HCl (solid to liquid ratio of 1:10) were mixed thoroughly by magnetic stirrers in a plastic flask and incubated for 24 h, followed by centrifugation (5000 rpm for 10 min) and filtration (20 μm, Waterman) to remove the soluble Ca^{2+}, Mg^{2+}, and other metal ions. A 0.5 M NaOH solution was used to dissolve the insoluble fraction consisting of the HAs, humin and ash. The pH of the solution was adjusted to 3 with 1 M HCl, and the final solid to liquid ratio was maintained at 1:10. After mixing and incubation for 24 h, the solution was centrifuged and filtered. The soluble portion was acidified to pH = 1 with dilute HCl, and the precipitates were centrifuged and filtered after 24 h and then oven-dried at 50 °C to

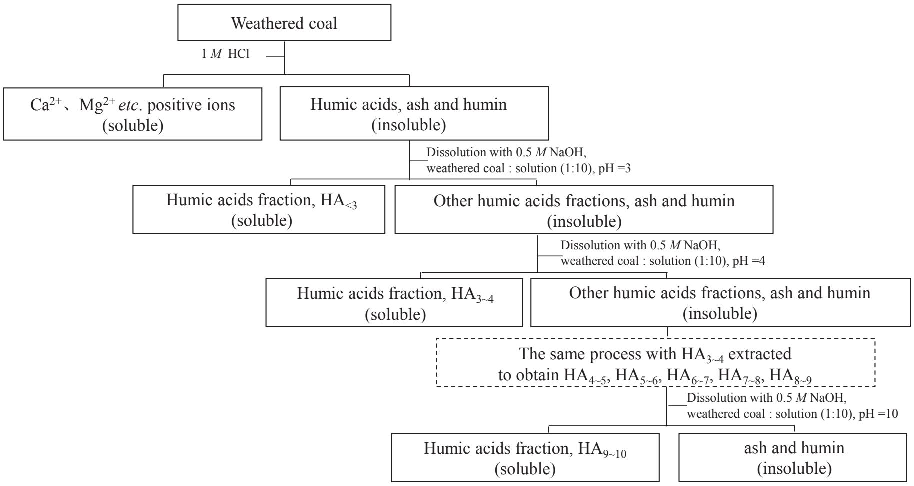

Fig. 1. Fractionation flowchart for the humic acids from Chinese weathered coal.

constant weight to obtain the dry HA fractions, which were labelled as $HA_{<3}$. The insoluble portion was dissolved as above, but the pH of the solution was adjusted to 4, and the rest of the procedure was repeated to obtain $HA_{3\sim4}$. The other fractions were obtained in a similar way, and the insoluble portion extracted from the solution with the highest pH (pH 10) was designated as humin and ash. The HA fractions were labelled as $HA_{(x-1)\sim(x)}$, where x is the solution pH. The HA fractions obtained were $HA_{3\sim4}$, $HA_{4\sim5}$, $HA_{5\sim6}$, $HA_{6\sim7}$, $HA_{7\sim8}$, $HA_{8\sim9}$, and $HA_{9\sim10}$. All the HA fractions were stored in polyethylene bags until further characterization, except for the $HA_{<3}$ fractions, which was too little to assay.

2.3. Characterization of the humic acid fractions

2.3.1. Elemental analysis

To determine the elemental compositions of the HA fractions, the contents of C, O, H and N in every HA fraction were analysed using a Vario Micro Cube Elementar (Elementar Analysensysteme GmbH, Germany). The analysis of each sample was performed twice to ensure the accuracy of the results.

2.3.2. Ultraviolet and visible light scanning

Ultraviolet and visible light spectra (220–900 nm) were collected using an Analytik SPECORD 200 PLUS UV/VIS spectrophotometer (Analytik Jena, Germany) for HA samples dissolved in a 0.05 M $NaHCO_3$ solution (with pH 8.3) at a concentration of 40 mg of HA per litre. The resultant solution was filtered to remove insoluble residues and then placed in a 1 cm quartz cell. The E_2/E_3 and E_4/E_6 ratios were calculated as the ratios of the optical density of HAs at 280 and 360, and 465 and 665 nm, respectively (Chen et al., 1977; Klavins and Purmalis, 2013).

2.3.3. Carboxylic groups and phenolic hydroxyl groups

Carboxylic groups and phenolic hydroxyl groups are the dominant oxygen-containing acidic functional groups in HAs and are an important indicator of humification (Rosell et al., 1989). The contents of carboxylic groups and total acidic groups were determined by the modified methods of Klavins and Purmalis (2013). The carboxylic group content was determined based on the Ca-acetate method. Twenty-milligram samples of HAs were weighed into 50-ml centrifuge tubes, and 25 ml of a 0.5 M $Ca(CH_3COO)_2$ solution was added under an N_2 atmosphere. The solutions were incubated for 48 h and shaken regularly every 2 h and then titrated to pH 8.3 with 0.1 M NaOH after filtration with phenolphthalein as an indicator under an N_2 atmosphere. The acidic groups were extracted by 0.05 M $Ba(OH)_2$ solution in a similar manner to the carboxylic groups, and after filtration, 10 ml of filtrate was removed. Then, 10 ml of 0.1 M HCl was added and mixed. Finally, the solutions were titrated to pH 8.3 with 0.1 M NaOH after filtration with phenolphthalein as an indicator under an N_2 atmosphere. The phenolic hydroxyl groups were calculated by the difference between the total acidic groups and the carboxylic groups.

2.3.4. Fourier transform infrared spectroscopy

Fourier transform infrared spectroscopy is an important method to determine the atom groups of materials, and it provides information about the existence and types of bonds (Kurková et al., 2004; Chai et al., 2013). A Tianjin Gangdong 650 FTIR spectrophotometer (TIANJINGANGDONG, China) was used to collect the infrared spectra. Approximately 2 mg of HA sample and 200 mg of spectrometry grade dried KBr were mixed under reduced pressure to obtain KBr pellets, which were analysed by the FTIR spectrophotometer. The FTIR spectra of humic acids were recorded in the 4000–400 cm^{-1} wavenumber range by taking the average of 32 scans with a resolution of 4 cm^{-1}. The spectra were corrected with the OMINC 8.2 software, with baseline correction and data smoothing correction. The region where the characteristic absorption peaks appeared was selected to calculate the second derivative of the absorbance using OMINC 8.2. Then, the results were used to conduct a principal component analysis (PCA) using SPSS 19.0.

2.3.5. Solid-state ^{13}C-nuclear magnetic resonance spectroscopy

To clarify the detailed distribution of the carbon functional groups of the HA fractions derived from weathered coal, solid-state ^{13}C NMR was conducted using a Bruker AVANCE III 400 spectrometer (Bruker, Switzerland) (Piccolo, 2002; Mao, Schmidt-Rohr, 2004; Longstaffe et al., 2016). ^{13}C cross polarization/total sideband suppression (CP/TOSS) and CP/TOSS with dipolar dephasing (DD) were selected to determine the functional group assignments of the HA fractions. Before detection, four-pulse total suppression of the sidebands (Dixon, 1982) was employed, and two-pulse phase-modulated decoupling was applied for optimum resolution. An NMR-tube was filled with approximately 100 mg of a HA fraction, and the NMR measurement was carried out with the following parameters: temperature: 293.7 K, NMR-tube diameter: 4 mm, speed of spinning: 5 kHz, number of scans: 2048, CP time: 1 ms, ^{1}H 90° pulse-length: 4 µs, and recycle delay time: 0.8 s. The

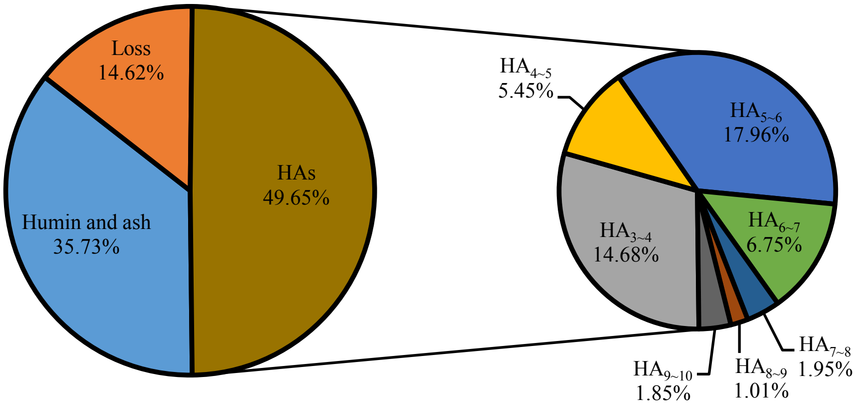

Fig. 2. Proportions of the humic acid fractions derived from Chinese weathered coal.

corresponding sub-spectra with signals of nonprotonated carbons and mobile groups, such as rotating CH_3, were obtained by ^{13}C CP/TOSS with 40 μs dipolar dephasing. The baseline correction and area integration in the special chemical shift regions of the spectra were performed with MestReNova 9.0.1 software.

3. Results

3.1. Yield distributions of the HA fractions in Chinese weathered coal

The extracted HAs accounted for 49.65% of the weathered coal weight: 35.73% was ash or humin, and the remaining 14.62% was attributed to loss during processing. Fig. 2 shows how the HAs were distributed in the different fractions. A significantly high cumulative percentage of HAs, 90.31%, was extracted in the acid to neutral (pH 3–7) extraction solutions. Within this pH range, the yields of the $HA_{3\sim4}$ and $HA_{5\sim6}$ factions accounted for 14.68% and 17.96% of the weathered coal weight, respectively, and were higher than the $HA_{4\sim5}$ and $HA_{6\sim7}$ yields.

3.2. Elemental composition of the extracted HA fractions

The results of the elemental analysis showed that the C content in the individual HA fractions ranged from 50.82% to 60.83%, the H content ranged from 3.71% to 5.00%, the N content ranged from 0.94% to 1.28%, and the O content ranged from 33.62% to 44.49% (Table 1). The N content of the HA fractions decreased with an increase in the extraction solution pH, whereas O showed an opposite and rough trend. In addition, the HA fractions extracted under acidic and neutral conditions (pH 3–7) had higher C and H contents than those extracted under alkaline conditions (pH 7–10). Other trends were observed for the ratios of the C, H and O contents: the O/C and O/H ratios showed an opposite trend to the C and H contents, and small variations were evident between the acidic and neutral HA fractions (pH 3–7) or the alkali fractions (pH 7–10). The H/C ratio exhibited irregular variation, with the fraction extracted at the lowest pH ($HA_{3\sim4}$) showing the highest H/C ratio of all of the HA fractions, with a secondary maximum at $HA_{7\sim8}$.

Table 1
Elemental composition and atomic ratios (normalized to ash-free samples) of the humic acid fractions derived from Chinese weathered coal.

Samples	C (%)	H (%)	N (%)	O (%)[b]	Atomic ratio		
					O/C[c]	H/C[c]	O/H[c]
$HA_{3\sim4}$	59.73[a]	5.00	1.28	33.99	0.43	1.00	0.42
$HA_{4\sim5}$	59.57	3.98	1.13	35.32	0.44	0.80	0.55
$HA_{5\sim6}$	60.51	4.01	1.10	34.38	0.43	0.80	0.54
$HA_{6\sim7}$	60.83	4.44	1.11	33.62	0.41	0.88	0.47
$HA_{7\sim8}$	52.33	3.98	0.97	42.72	0.61	0.91	0.67
$HA_{8\sim9}$	50.82	3.71	0.98	44.49	0.66	0.88	0.75
$HA_{9\sim10}$	55.89	3.97	0.94	39.20	0.53	0.85	0.62

[a] The mean of three analyses.
[b] Calculated as the difference in the sum of the other element contents and 100%.
[c] The atomic ratio.

3.3. Ultraviolet and visible light spectra and the content of acidic functional groups

UV–Vis spectra of the HA provide basic chemical bonding structural information about the HA fractions (Chen et al., 1977; Traina et al., 1990). Fig. 3 shows the ultraviolet and visible light spectra. All of the extracted HA fractions showed monotonically decreasing absorbance with increasing wavelength, whereas the absorbance decreased more quickly in the ultraviolet region compared to the visible region. No distinct peak was evident in the spectra of the HA fractions. The spectra showed clear absorbance differences at 220 nm, but all approached zero at 900 nm, suggesting slight differences in the bonds among fractions. These results agree with Fujitake's results (1999) for HA fractions extracted from the soil. In addition, a stepwise reduction at 280 nm was seen

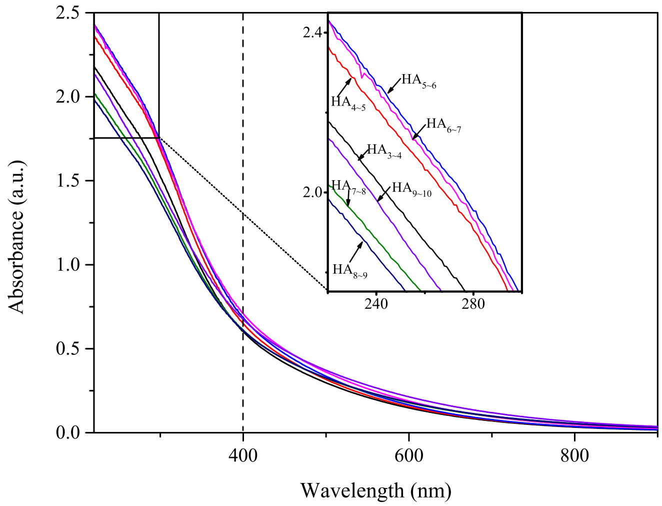

Fig. 3. UV–Vis spectra of the humic acid fractions derived from Chinese weathered coal.

Table 2
Acidic functional group contents and E_2/E_3 and E_4/E_6 ratios of the humic acid fractions derived from Chinese weathered coal.

Samples	Ratios		Acidic groups			
	E_2/E_3	E_4/E_6	Total acidic groups (mmol/g)	Carboxylic groups (mmol/g)	Phenolic hydroxyl groups[b] (mmol/g)	Carboxylic groups/Total acidic groups (%)
HA$_{3\sim4}$	1.97[a]	4.12	6.76	4.71	2.05	69.67
HA$_{4\sim5}$	2.00	4.19	6.53	4.47	2.06	68.45
HA$_{5\sim6}$	1.95	4.21	6.48	4.32	2.16	66.67
HA$_{6\sim7}$	1.91	3.73	5.71	3.38	2.33	59.19
HA$_{7\sim8}$	1.87	3.33	5.22	3.20	2.02	61.30
HA$_{8\sim9}$	1.85	3.27	4.82	2.69	2.13	55.81
HA$_{9\sim10}$	1.78	3.08	4.78	2.30	2.48	48.12

[a] The mean of three analyses.
[b] Calculated as the difference of the total acidic groups and carboxylic groups.

in the spectra of HA$_{3\sim4}$, HA$_{4\sim5}$, HA$_{5\sim6}$ and HA$_{6\sim7}$, which is an indication of a high degree of coalification and aromatization (Zheng, 1991). The “slope” of the absorption curves could be quantitatively described by the ratios of the absorbance at 280 and 360 (E_2/E_3) and 465 and 665 nm (E_4/E_6), which have been suggested to be negatively correlated with the aromaticity and molecular weight of HAs (Chen et al., 1977; Klavins and Purmalis, 2013). These ratios are given in Table 2. The ratios roughly decreased with increasing extract pH. The HAs extracted at a higher pH had lower E_2/E_3 and E_4/E_6 ratios, especially the HA$_{6\sim7}$, HA$_{7\sim8}$, HA$_{8\sim9}$, and HA$_{9\sim10}$ fractions. No significant differences were evident among the E_2/E_3 ratios of the HA$_{3\sim4}$, HA$_{4\sim5}$, and HA$_{5\sim6}$ fractions. The result was found for the E_4/E_6 ratios.

The contents of total acidic groups and carboxyl groups in the HA fractions decreased with an increasing pH of the extraction solution (Table 2). The contents of total acidic groups and carboxyl groups in HA$_{3\sim4}$ were higher than those in HA$_{9\sim10}$ by 0.54 and 1.05 times, respectively. However, the contents of phenolic hydroxyl groups in all of the HA fractions were in the range of 2.05–2.48 mmol/g and had relatively small variations, indicating no significant difference in the phenolic hydroxyl contents among various HA fractions. The ratios of carboxylic groups to total acidic groups were calculated to analyse the trends in the oxygen-containing acidic functional groups. The percentages showed similar changes in the total acidic groups and carboxyl groups, that is, the proportion of phenolic hydroxyl groups exhibited an increasing trend with an increasing pH of the extraction solution.

3.4. *Fourier transform infrared-principal component analysis*

The FTIR spectra of HA fractions are shown in Fig. 4. All of the spectra had similar primary absorption bands. The common peaks included (a) a broad absorption peak at 3500–3400 cm^{-1} attributed to C=C stretching in aromatic rings and O-H stretching in alcohols and phenols, (b) a comparatively sharp absorption peak at 1618 cm^{-1} arising from the skeletal vibration of C=C in aromatic rings or C=O stretching in chinone, and (c) paired peaks at 1031 and 1010 cm^{-1} due to C-O stretching of primary alcohols or polysaccharide and Si-O stretching arising from impurities. Some characteristic peaks appeared in the spectra of the HA$_{7\sim8}$, HA$_{8\sim9}$ and HA$_{9\sim10}$ fractions at 3689–3615 and 1390 cm^{-1}, which were attributed to the stretching vibration of dissociative O-H and C-O stretching/O-H in-plane bending in phenols. The spectra of all of the HA fractions had peaks at 1707 and 1252 cm^{-1}. However, the vibration intensity of the HA fractions extracted from the pH 6–7 solution was weaker than those extracted under acidic conditions (pH 3–4, 4–5, and 5–6) but stronger than those extracted under alkaline conditions (pH 7–8, 8–9, and 9–10). The peak at 1707 cm^{-1} was due to the C=O stretching of carboxylic acid (COOH) and other carbonyl groups, including aldehydes. C-O stretching and O-H deformation in the carboxyl groups resulted in a peak at 1252 cm^{-1}, which was probably attributed to C-O stretching of aromatic ethers and phenol as well, indicating the likely presence of carboxyl groups, alcohol or phenol.

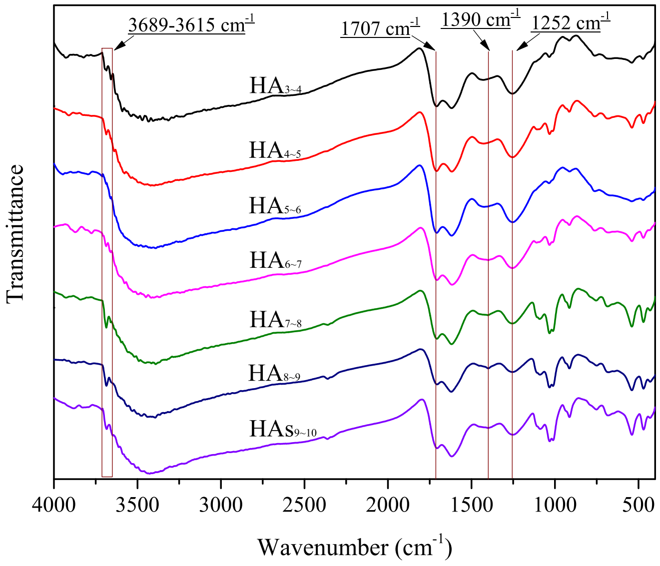

Fig. 4. FTIR spectra of the humic acid fractions derived from Chinese weathered coal.

The spectral differences can be investigated by PCA (Goncalves et al., 1998; De Benedetto et al., 2005). However, Benar et al. (1999) proved that complex changes cannot be determined by a PCA of the total spectrum. Thus, in most current research, the region where the absorption peaks are concentrated is selected for FTIR-PCA (Abbas et al., 2008; Foulks et al., 2013). In this study, the second derivative of the absorbance at 1800–860 cm^{-1} consisting of 488 data points was used for FTIR-PCA. The results of FTIR-PCA indicated that Component 1 and Component 2, respectively, accounted for 70.29% and 9.71% of the variation and for 80.00% of the total variance. A scatter plot of the scores of Component 1 and Component 2 is shown in Fig. 5. The data points are unevenly distributed in the different quadrants, indicating that the substances studied were distinct. HA$_{3\sim4}$, HA$_{4\sim5}$ and HA$_{5\sim6}$, which are soluble in extraction solutions with low pH, were concentrated in the second quadrant. The fractions HA$_{7\sim8}$, HA$_{8\sim9}$ and HA$_{9\sim10}$ had positive values for Component 1. The first two fractions were in the first quadrant and the last fraction in the fourth quadrant. Only HA$_{6\sim7}$ was in the third quadrant. Therefore, according to the distribution in Fig. 5, the studied fractions could be classified into three species. Based on these results, HA$_{3\sim4}$, HA$_{6\sim7}$, and HA$_{9\sim10}$ were used as representatives to analyse the differences between fractions.

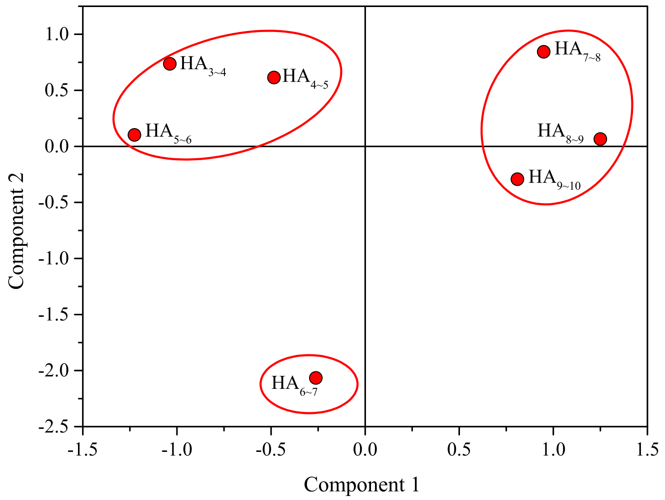

Fig. 5. Score plots of the first two principal components (Component 1 × Component 2) of the FTIR-PCA using the second derivative spectra at 1800–860 cm^{-1} of the humic acid fractions derived from Chinese weathered coal. The points represent the corresponding HA fractions.

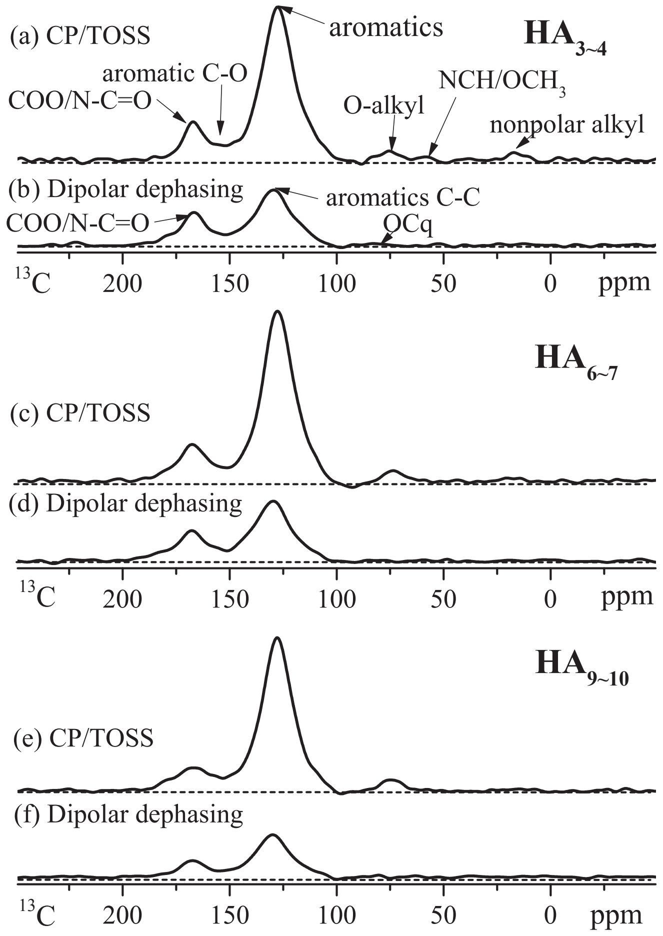

Fig. 6. NMR spectra of the humic acid fractions derived from Chinese weathered coal bsy unselective CP/TOSS (a, c, e) and dipolar-dephased techniques (b, d, f).

3.5. Solid-state ^{13}C-nuclear magnetic resonance spectra

Fractions HA$_{3\sim4}$, HA$_{6\sim7}$, and HA$_{9\sim10}$ were selected for a solid-state ^{13}C CP/TOSS NMR analysis according to the results of the FTIR-PCA. The spectra are shown in Fig. 6: plots a, c, e are for unselective CP/TOSS and plots b, d, f are for dipolar-dephased techniques (DD). Specific assignments of different functional groups were calculated and analysed based on the spectra and data obtained by following the methods of Mao et al. (2008) and Zhang et al. (2015). Furthermore, because of the low concentrations of 0–44 and 44–64 ppm in this study, the two neighbouring chemical shift regions were merged into one, representing the functional groups of alkyl C. The nonprotonated carbon, OCq (nonprotonated O-alkyl carbons) and aromatic C-C (nonprotonated aromatic carbons), were separated by comparing the differences between CP/TOSS and CP/TOSS with DD (Table 3). As shown in Fig. 6, the highest abundance in all the spectra occurred in the chemical shift region of 93–143 ppm, suggesting that aromatics were the predominant form of carbon. The aromatic functional groups accounted for more than 80% of the carbon when aromatic C-O was also taken into consideration. Carbon in the chemical shift region of 163–190 ppm belonging to COO/N-C=O was the next most abundant and was approximately 10%. In addition, the peak of COO/N-C=O in HA$_{9\sim10}$ had a weaker intensity than those in HA$_{3\sim4}$ and HA$_{6\sim7}$. Other functional groups accounted for less than 10% of the carbon, but some small changes were still observed in these regions. Some small alkyl C bands (0–64 ppm) were evident in HA$_{3\sim4}$, but these bands were not present in the spectra of HA$_{6\sim7}$ and HA$_{9\sim10}$.

The HA$_{3\sim4}$, HA$_{6\sim7}$, and HA$_{9\sim10}$ fractions had some differences in the various chemical shift regions (Table 3). Some corresponding changes in abundances with increasing pH of the extraction solution were noted. The abundance of OCH, the protonated carbon in O-alkyl C, increased unevenly with an increasing pH of the extraction solution. The proportion of O-alkyl C in HA$_{9\sim10}$ was 3.56%, approximately twofold higher than those in HA$_{3\sim4}$ and HA$_{6\sim7}$. The relative proportions of the aromatic C-H, protonated aromatic carbon, in HA$_{3\sim4}$, HA$_{6\sim7}$ and HA$_{9\sim10}$ were 49.47%, 44.35% and 39.04%, respectively, remarkably exhibiting a descending order with the elevated pH of the extraction solutions, but the aromatic C-C had an opposite trend. However, the total proportions of nonpolar aromatics (aromatic C-H and aromatic C-O) in HA$_{3\sim4}$, HA$_{6\sim7}$ and HA$_{9\sim10}$ (77.13%, 77.42%, and 77.21%, respectively) had near-negligible variation. In addition, there was an inconsistent decrease or increase in the other chemical shift regions. The proportion of alkyl C and aromatic C-O in HA$_{3\sim4}$ had maxima of 1.60% and 9.31%, respectively. The maximum COO/N-C=O was found in HA$_{6\sim7}$, slightly exceeding that in HA$_{3\sim4}$ and HA$_{9\sim10}$. The aromaticity index of HA$_{6\sim7}$ was higher than those of HA$_{3\sim4}$ and HA$_{9\sim10}$.

4. Discussion

4.1. The characteristics of the pH-derived HA fractions from Chinese weathered coal

This study found that more than 90% of the HAs were extracted at acidic and neutral (pH 3–7). This is not in accord with the results of Fujitake et al. (1998), who reported that the yields of fulvic acid and the humic acid fractions extracted with acidic to neutral solutions were equal to or slightly higher than those extracted with pyrophosphate buffer solution at alkaline pH (pH 9–13). You et al. (2006) investigated different types of soils and found that a significant amount of typical soil humic substances were soluble in an extraction solution with a pH between 5 and 7. Although the “predominant” HA fractions are extracted from acidic and neutral (pH 3–7) solutions, the HA yields extracted at this pH reported in the literature were significantly lower than in the present study. This discrepancy can be explained by several observations. Fujitake et al. (1998) and You et al. (2006) selected soil as the raw material,

Table 3
The assignment of functional groups in the different chemical shift regions and their relative proportions determined by CP/TOSS and dipolar-dephased techniques in the humic acid fractions derived from Chinese weathered coal.

Samples	Assignment at different chemical shift regions (ppm) and their relative proportions (%)								Aromaticity index[b]
	0–64	64–93		93–143		143–163	163–190	190–220	
	Alkyl C	O-alkyl		Aromatics		Aromatic C–O	COO/N–C=O	Ketones/aldehydes	
		OCH	OCq[a]	C–H	C–C[a]				
$HA_{3\sim4}$	1.60	1.76	0.20	49.47	27.66	9.31	10.02	0.00	0.96
$HA_{6\sim7}$	0.16	1.86	0.00	44.35	33.07	8.90	11.78	0.02	0.98
$HA_{9\sim10}$	0.46	3.44	0.12	39.04	38.17	9.20	9.58	0.08	0.96

[a] Determined by CP/TOSS with dipolar-dephased techniques.
[b] Aromaticity index = (all aromatic C)/(alkyl C + O-alkyl C + all aromatic C).

whereas in this study, the source material was weathered coal, which has a comparatively higher aromaticity (Zheng, 1991). Additionally, this study used pre-processing via acidification to remove metal ions, which was not performed in the previous studies. It is likely that the acidification introduced more H^+ ions, which disturbed the inherent distribution of HA fractions (Cheng, 2003). Furthermore, the acidification could break chemical bonds, especially hydrogen bonds, which led to increased HA solubility in the acidic and neutral (pH 3–7) extraction solutions.

The E_4/E_6 ratio of the HA fractions in this study were also different from those in previous studies. In this study, the HA E_4/E_6 ratio was 3.08–4.21, but it was previously reported to be 6–9 (Fujitake et al., 1998; Dong et al., 2008; Klavins and Purmalis, 2013; Novák et al., 2015), suggesting that compared with the HAs used in the literature reports, the HA fractions in this study had higher aromaticity, condensation and molecular weight (Chen et al., 1977; Chin et al., 1994). The FTIR and solid-state ^{13}C NMR spectra showed significant characteristic peaks at 3500–3400 cm^{-1} and 200–100 ppm, respectively, which verified that most of the carbon of the HA fractions existed as aromatic carbon and that aromatic rings formed the physical and chemical “backbone” of the HA fractions in this study. More than 80% of the carbon was aromatic carbon. In the literature, the proportions of aromatic carbon in humic acids extracted from lignite and soil were below 60% (Mao et al., 2007; Dong et al., 2009; Khalaf et al., 2014; Kawasaki et al., 2015). The difference in the origins was attributed to the high aromatic C in this study. Weathered coal is found either on the surface of the earth or buried in shallow coal beds, therefore, it is more conducive to oxidation and humification, which entails the conversion of alkyl and O-alkyl C to aromatic C (Zheng, 1991).

4.2. *The differences between the HA fractions derived from Chinese weathered coal*

Fujitake et al. (1998) found that the properties of the HA fractions from the same soil varied much less than those extracted from different soils. In this study, the differences between the HA fractions were relatively small, in agreement with Fujitake et al. (1998); nevertheless, some fine structural and compositional differences were evident in our data. The E_2/E_3 and E_4/E_6 ratios of $HA_{3\sim4}$, $HA_{6\sim7}$, and $HA_{9\sim10}$ showed a decreasing order, and it was suggested that the HA fractions extracted at higher pH had a higher degree of aromatic polycondensation and a higher molecular mass (Chen et al., 1977; Klavins and Purmalis, 2013). In addition, the H/C ratios showed a similar tendency to the E_2/E_3 and E_4/E_6 ratios, indicating a decrease of the aliphatic structure and an increase of the aromatic structure (Dong et al., 2008). The above is in agreement with the results of Fujitake et al. (1998, 2003), who reported that the particle size and the H/C ratios of HA fractions gradually and regularly increased with an increase of the pH (5–13) of the extraction solution. Compared with $HA_{6\sim7}$ and $HA_{9\sim10}$, $HA_{3\sim4}$ had a significantly higher C content, suggesting a higher abundance of alkyl C and O-alkyl C but a lower abundance of aromatic C and carbonyl C (Mahieu et al., 1999; Chen and Chiu, 2003). However, the solid-state ^{13}C NMR indicated that the highest aromaticity was present in $HA_{6\sim7}$, which did not agree with the above prediction. However, the abundances of alkyl C and O-alkyl C (O-CH and OCq) were at a minimum (0.16% and 1.86%, respectively) in $HA_{6\sim7}$ instead of $HA_{9\sim10}$. Similarly, the proportions of nonpolar aromatic C and carbonyl C (COO/N-C=O) were at a maximum in $HA_{6\sim7}$. Therefore, $HA_{9\sim10}$ was an exception to the conventional rules. It was suggested that the ash mixed with $HA_{9\sim10}$ interfered with the regular values, and the limited differences in the HA fractions were covered up by ash. In addition, based on an acid-base titration, the contents of the total acidic groups and carboxyl groups in the HA fraction showed a decreasing order with an increase of the pH of the extraction solution (Table 2), in accordance with the NMR assignments of Fujitake et al. (2003). However, the proportion of COO/N-C=O by NMR in this study was inconsistent with the carboxyl group content determined by acid-base titration. The NMR assignment showed a similar COO/N-C=O proportion in the HA fractions, and the abundances of COO/N-C=O in $HA_{6\sim7}$ were higher than in $HA_{3\sim4}$ and $HA_{9\sim10}$. The reason for the different trends of COO/N-C=O in $HA_{3\sim4}$ and $HA_{6\sim7}$ was attributed to the different detection technologies, which hid the slight differences between the HA fractions, or because the fractionation method caused inaccuracy of the acid-base titration when the functional groups were analysed.

Despite the disagreement of the results from different methods, the relatively higher aromaticity and more abundant COO/N-C=O in the $HA_{6\sim7}$ fraction was definite. Dong et al. (2008) argued that humic acids with abundant aromatics could reduce ammonia volatilization by inhibiting urease activity at pH 8 and could ensure the nitrogen supply by protecting urease from oxidation in the later stages. This implies that a high aromatic content in HAs enhances urea utilization. In addition, the acidic groups, especially the carboxyl groups of the HA fractions can incorporate the -NH_2 of urea to produce highly stable humic-urea that inhibits urea decomposition (Liang et al., 1996; Dong et al., 2009; Tan, 2014). This provided a prospective use for the humic acids derived from weathered coal, especially $HA_{6\sim7}$.

The nonprotonated C calculated by CP/TOSS with DD is located in the chemical shift regions of 64–93 ppm and 93–143 ppm. When compared with nonprotonated aromatic C (aromatic C-C), the relative proportion of nonprotonated O-alkyl (OCq) was very low in this study, so OCq was not taken into consideration in the analysis of nonprotonated C. The concentration of nonprotonated aromatic carbon can represent the humification of organic matter (Stevenson, 1994; Mahieu et al., 2002; Zhang et al., 2015). In this study, the relative proportions of nonprotonated aromatic carbon (aromatic C-C) in the chemical shift region of 93–143 ppm in $HA_{3\sim4}$,

$HA_{6\sim7}$ and $HA_{9\sim10}$ were 27.66%, 33.07% and 38.17%, respectively, exhibiting a remarkable increase with increasing pH. In addition, Mao and Schmidt-Rohr (2004) reported that the proportion of nonprotonated aromatic carbon increased with an increasing in the size of the fused aromatic rings and could therefore be used to estimate the typical size of the polycyclic aromatic components in highly aromatic natural organic matter. HAs with very few non-protonated C structures (nonprotonated O-alkyl and aromatic C-C) are generally considered more easily degradable (Miltner and Zech, 1998). Therefore, the HA fractions extracted at high pH are likely to contain structures with more fused aromatic rings and could be more resistant to decomposition. Zhang et al. (2015) demonstrated that after glucose addition, the relative abundance of protonated O-alkyl C (OCH) and aromatic C-H groups in soil organic matter decreased along with the incubation time, and the OCq and aromatic C-C groups were higher, suggesting that more protonated C was replaced by nonprotonated C. Thus, the HA fractions extracted at high pH were more likely to have a prior formation period.

As shown in the above experimental results, the carboxyl group content of the HA fractions varied irregularly with an increase in the pH of the extraction solution in this study, possibly because the acidic functional groups are not the only factor that determines the dissociation behaviour of the HAs, and dissociation is also affected by other functional groups (Klučáková, 2016). Klučáková and Kalina (2015) has also suggested that the chemical structure of the molecules determines the dissociation of functional groups at different pHs. In the HAs derived from Chinese weathered coal, more than 80% of the carbon was aromatic, so the aromatic structure is more likely to affect fractionation. In this study, when the pH of extraction solutions increased, the proportions of aromatic C-H and aromatic C-O in HA fractions showed a descending and ascending trend, respectively. Thus, in a similar manner to the acidic functional groups that predominate in the pH-based fractionation of HAs derived from lignite and soil (Bakina and Orlova, 2012; Klučáková and Kalina, 2015), the dissociation of protonated aromatic groups might be an important factor in the pH-fractionation of HAs derived from Chinese weathered coal. However, further studies are necessary to confirm this hypothesis.

Therefore, due to the specific original materials and fractionation methods employed, the HAs from the weathered coal in this study were mostly distributed in acidic and neutral (pH 3–7) solutions. The results indicated that most of the C in the HA was aromatic (Mao, Schmidt-Rohr, 2004; Mao et al., 2007). The $HA_{6\sim7}$ fraction had the highest aromaticity and COO/N-C=O groups. In addition, compared with $HA_{3\sim4}$ and $HA_{9\sim10}$ fractions, the non-protonated C in the $HA_{6\sim7}$ fraction was moderate, indicating resistance to decomposition (Zhang et al., 2015). The results indicated that the $HA_{6\sim7}$ fraction was stable and had the greatest potential to improve nitrogen fertilizer use efficiency (Dong et al., 2008, 2009).

5. Conclusion

We have demonstrated that the HAs of weathered coal can be fractionated by adjusting the pH of the extraction solutions with dilute NaOH and HCl and that the properties of the HA fractions show roughly consistent changes. More than 90% of the HAs from weathered coal were extracted from acidic to neutral solutions (pH 3–7). In these HA fractions, the proportions of aromatic C was greater than 80%, suggesting that the HA fractions in this study had structures characterized by higher condensation and molecular weight. Compared with the HA fractions from acidic or alkaline solutions, the HA fractions extracted from neutral solutions had the highest aromaticity index and more abundant COO/N-C=O functional groups, indicating a greater capacity to inhibit the urease activity, which would protect urease from oxidation in the later stages and allow for the incorporation of the $-NH_2$ of urea. Therefore, the HA fractions extracted from neutral solutions have an advantage in the improvement of urea utilization. In addition, the proportion of nonprotonated C in $HA_{6\sim7}$ is moderate, a sign of resistance to decomposition and of prior formation. From this investigation, it is clear that weathered coal is a good source of humic acids, particularly the fractions extracted at neutral pH.

Acknowledgements

The authors acknowledge the financial support provided by the National Natural Science Foundation of China (NSFC, Grant No. 31601827) and Key Technologies R&D Program of China during the 12th and 13th Five-Year Plan period (Grant No. 2011BAD11B05 and 2016YFD0200402).

References

Abbas, O., Rebufa, C., Dupuy, N., Kister, J., 2008. FTIR-Multivariate curve resolution monitoring of photo-Fenton degradation of phenolic aqueous solutions: comparison with HPLC as a reference method. Talanta 77, 200–209.

Asakawa, D., Kiyota, T., Yanagi, Y., Fujitake, N., 2008. Optimization of conditions for high-performance size-exclusion chromatography of different soil humic acids. Anal. Sci. 24, 607–613.

Bakina, L.G., Orlova, N.E., 2012. Special features of humus acids extraction from soils by sodium pyrophosphate solutions of different alkalinity. Eur. Soil Sci. 45, 392–398.

Benar, P., Gonçalves, A.R., Mandelli, D., Ferreira, M.M., Schuchardt, U., 1999. Principal component analysis of the hydroxymethylation of sugarcane lignin: a time-depending study by FTIR. J. Wood Chem. Technol. 19, 151–165.

Brigante, M., Zanini, G., Avena, M., 2009. Effect of pH, anions and cations on the dissolution kinetics of humic acid particles. Coll. Surf. A 347, 180–186.

Canellas, L.P., Piccolo, A., Dobbss, L.B., Spaccini, R., Olivares, F.L., Zandonadi, D.B., Façanha, A.R., 2010. Chemical composition and bioactivity properties of size-fractions separated from a vermicompost humic acid. Chemosphere 78, 457–466.

Chai, X.L., Hao, Y.X., Liu, G.X., Zhao, X., Zhao, Y.C., 2013. Spectroscopic studies of the effect of aerobic conditions on the chemical characteristics of humic acid in landfill leachate and its implication for the environment. Chemosphere 91, 1058–1063.

Chen, J.S., Chiu, C.Y., 2003. Characterization of soil organic matter in different particle-size fractions in humid subalpine soils by CP/MAS ^{13}C NMR. Geoderma 117, 129–141.

Chen, Y., Senesi, N., Schnitzer, M., 1977. Information provided on humic substances by E_4/E_6 ratios. Soil Sci. Soc. Am. J. 41, 352–358.

Cheng, S., 2003. The activation and passivation of humic substances & their application on green fertilizer. Humic Acid. 5, 1–14 (in Chinese).

Chin, Y.P., Aiken, G., O'Loughlin, E., 1994. Molecular weight, polydispersity, and spectroscopic properties of aquatic humic substances. Environ. Sci. Technol. 28, 1853–1858.

De Benedetto, G.E., Fabbri, B., Gualtieri, S., Sabbatini, L., Zambonin, P.G., 2005. FTIR-chemometric tools as aids for data reduction and classification of pre-Roman ceramics. J. Cult. Herit. 6, 205–211.

Dixon, W.T., 1982. Spinning-sideband-free and spinning-sideband-only NMR spectra in spinning samples. J. Chem. Phys. 77, 1800–1809.

Dong, L.H., Yang, J.S., Yuan, H.L., Wang, E.T., Chen, W.X., 2008. Chemical characteristics and influences of two fractions of Chinese lignite humic acids on urease. Eur. J. Soil Biol. 44, 166–171.

Dong, L.H., Córdova-Kreylos, A.L., Yang, J., Yuan, H.L., Scow, K.M., 2009. Humic acids buffer the effects of urea on soil ammonia oxidizers and potential nitrification. Soil Biol. Biochem. 41, 1612–1621.

Foulks, G.N., Borchman, D., Yappert, M., Kakar, S., 2013. Topical azithromycin and oral doxycycline therapy of meibomian gland dysfunction: a comparative clinical and spectroscopic pilot study. Cornea 32, 44–53.

Fujitake, N., Kusumoto, A., Tsukamoto, M., Kawahigashi, M., Suzuki, T., Otsuka, H., 1998. Properties of soil humic substances in fractions obtained by sequential extraction with pyrophosphate solutions at different pHs: I. yield and particle size distribution. Soil Sci. Plant Nutr. 44, 253–260.

Fujitake, N., Kusumoto, A., Tsukamoto, M., Noda, Y., Suzuki, T., Otsuka, H., 1999. Properties of soil humic substances in fractions obtained by sequential extraction with pyrophosphate solutions at different pHs: II. Elemental composition and UV-VIS spectra of humic acids. Soil Sci. Plant Nutr. 45, 349–358.

Fujitake, N., Kusumoto, A., Yanagi, Y., Suzuki, T., Otsuka, H., 2003. Properties of soil humic substances in fractions obtained by sequential extraction with pyrophosphate solutions at different pHs: III. FT-IR and ^{1}H NMR spectra of humic acids. Soil Sci. Plant Nutr. 49, 347–353.

Goncalves, A.R., Esposito, E., Benar, P., 1998. Evaluation of Panus tigrinus in the delignification of sugarcane bagasse by FTIR-PCA and pulp properties.

J. Biotechnol. 66, 177–185.

Hayes, M.H.B., Wilson, W.R., 1997. Humic Substances, Peats and Sludges. Royal Scoiety of Chemistry, Cambridge.

He, J., Yan, L., Yang, K., Ma, M.H., Liu, Y., Cui, G.F., 2003. Study on component and character of humic acids from different sources. Chin. J. Soil Sci. 26, 343–345 (in Chinese).

Kawasaki, S., Ikeya, K., Sugiura, Y., Watanabe, A., 2015. Changes in the composition of humic acids in various upland field soils with a continuous application of an organic amendment as revealed by fractional precipitation analysis. Soil Sci. Plant Nutr. 61, 450–460.

Khalaf, M.M., Chilom, G., Rice, J.A., 2014. Comparison of the effects of self-assembly and chemical composition on humic acid mineralization. Soil Biol. Biochem. 73, 96–105.

Kipton, H., Powell, J., Town, R.M., 1992. Solubility and fractionation of humic acid; effect of pH and ionic medium. Anal. Chim. Acta 267, 47–54.

Klavins, M., Purmalis, O., 2013. Properties and structure of raised bog peat humic acids. J. Mol. Struct. 1050, 103–113.

Klučáková, M., 2016. Characterization of pH-fractionated humic acids with respect to their dissociation behaviour. Environ. Sci. Pollut. R. 23, 7722–7731.

Klučáková, M., Kalina, M., 2015. Composition, particle size, charge, and colloidal stability of pH-fractionated humic acids. J. Soils Sediments 15, 1–9.

Klučáková, M., Pekař, M., 2005. Solubility and dissociation of lignitic humic acids in water suspension. Coll. Surf. A 252, 157–163.

Kurková, M., Klika, Z., Kliková, C., Havel, J., 2004. Humic acids from oxidized coals: I. Elemental composition, titration curves, heavy metals in HA samples, nuclear magnetic resonance spectra of HA and infrared spectroscopy. Chemosphere 54, 1237–1245.

Li, H., Shao, H.B., Li, W.X., Bi, R.T., Bai, Z.K., 2012. Improving soil enzyme activities and related quality properties of reclaimed soil by applying weathered coal in opencast-mining areas of the Chinese loess plateau. Clean. Soil Air Water 40, 233–238.

Liang, Z.C., Wu, L.P., Cheng, S.X., 1996. Study on the action mechanism of humic acids derived from coal and urea & the composition and structure of reaction products. Humic Acid. 3, 8–10 (in Chinese).

Longstaffe, J.G., Courtier-Murias, D., Simpson, A.J., 2016. A nuclear magnetic resonance study of the dynamics of organofluorine interactions with a dissolved humic acid. Chemosphere 145, 307–313.

Mahieu, N., Randall, E.W., Powlson, D.S., 1999. Statistical analysis of published carbon-13 CPMAS NMR spectra of soil organic matter. Soil Sci. Soc. Am. J. 63, 307–319.

Mahieu, N., Olk, D.C., Randall, E.W., 2002. Multinuclear magnetic resonance analysis of two humic acid fractions from lowland rice soils. J. Environ. Qual. 31, 421–430.

Mao, J.D., Schmidt-Rohr, K., 2004. Accurate quantification of aromaticity and nonprotonated aromatic carbon fraction in natural organic matter by ^{13}C solid-state nuclear magnetic resonance. Environ. Sci. Technol. 38, 2680–2684.

Mao, J.D., Fang, X.W., Schmidt-Rohr, K., Carmo, A.M., Hundal, L.S., Thompson, M.L., 2007. Molecular-scale heterogeneity of humic acid in particle-size fractions of two Iowa soils. Geoderma 140, 17–29.

Mao, J.D., Olk, D.C., Fang, X.W., He, Z.Q., Schmidt-Rohr, K., 2008. Influence of animal manure application on the chemical structures of soil organic matter as investigated by advanced solid-state NMR and FT-IR spectroscopy. Geoderma 146, 353–362.

Mao, J.D., Schimmelmann, A., Mastalerz, M., Hatcher, P.G., Li, Y., 2010. Structural features of a bituminous coal and their changes during low-temperature oxidation and loss of volatiles investigated by advanced solid-state NMR spectroscopy. Energy Fuel 24, 2536–2544.

Mei, M.T., Cui, J.Z., 1994. Analysis of coal-forming plants in underlying coal-bearing member of Holinhe Formation, Inner Mongolia. Coal Geol. China 6, 19–21 (in Chinese).

Miltner, A., Zech, W., 1998. Carbohydrate decomposition in beech litter as influenced by aluminium, iron and manganese oxides. Soil Biol. Biochem. 30, 1–7.

Nardi, S., Pizzeghello, D., Muscolo, A., Vianello, A., 2002. Physiological effects of humic substances on higher plants. Soil Biol. Biochem. 34, 1527–1536.

Nardi, S., Muscolo, A., Vaccaro, S., Baiano, S., Spaccini, R., Piccolo, A., 2007. Relationship between molecular characteristics of soil humic fractions and glycolytic pathway and krebs cycle in maize seedlings. Soil Biol. Biochem. 39, 3138–3146.

Novák, F., Šestauberová, M., Hrabal, R., 2015. Structural features of lignohumic acids. J. Mol. Struct. 1093, 179–185.

Piccolo, A., 2002. The supramolecular structure of humic substances: a novel understanding of humus chemistry and implications in soil science. Adv. Agron. 75, 57–134.

Rosell, R.A., Andriulo, A.E., Schnitzer, M., Crespo, M.B., Miglierina, A.M., 1989. Humic acids properties of an Argiudoll soil under two tillage systems. Sci. Total Environ. 81, 391–400.

Stevenson, F.J., 1994. Humus Chemistry: Genesis, Composition, Reactions, second ed. Wiley, New York.

Tan, K.H., 2014. Humic Matter in Soil and the Environment: Principles and Controversies, second ed. CRC Press, Florida.

Traina, S.J., Novak, J., Smeck, N.E., 1990. An ultraviolet absorbance method of estimating the percent aromatic carbon content of humic acids. J. Environ. Qual. 19, 151–153.

You, S.J., Thakali, S., Allen, H.E., 2006. Characteristics of soil organic matter (SOM) extracted using base with subsequent pH lowering and sequential pH extraction. Environ. Int. 32, 101–105.

Yuan, L., Zhao, B.Q., Li, Y.T., Li, J., 2015. A Method of Separation of Humic Acids by pH and its Application. CN, Patent, 201410026137 (in Chinese).

Zhang, Y.L., Yao, S.H., Mao, J.D., Olk, D.C., Cao, X.Y., Zhang, B., 2015. Chemical composition of organic matter in a deep soil changed with a positive priming effect due to glucose addition as investigated by ^{13}C NMR spectroscopy. Soil Biol. Biochem. 85, 137–144.

Zheng, P., 1991. The Application and Production of Peat Humic Acids. Chemical Industry Press, Beijing (in Chinese).